Decreased Thermal Conductivity of Polyethylene Chain Influenced by Short Chain Branching

Danchen Luo
School of Electrical and Power Engineering,
China University of Mining and Technology,
Xuzhou 221116, China

Congliang Huang[1]
School of Electrical and Power Engineering,
China University of Mining and Technology,
Xuzhou 221116, China;
Department of Mechanical Engineering,
University of Colorado,
Boulder, CO 80309-0427
e-mail: huangcl@cumt.edu.cn

Zun Huang
School of Electrical and Power Engineering,
China University of Mining and Technology,
Xuzhou 221116, China

In this paper, we have studied the effect of short branches (side chains) on the thermal conductivity (TC) of a polyethylene (PE) chain. With a reverse nonequilibrium molecular dynamics (RNEMD) method, TCs of the pristine PE chain and the PE-ethyl chain are simulated and compared. It shows that the branch has a positive effect to decrease the TC of a PE chain. The TC of the PE-ethyl chain decreases with the number density increase of branches, until the density becomes larger than about eight ethyl per 200 segments, where the TC saturates to be only about 40% that of a pristine PE chain. Because of different weights, different branches will cause a different decrease of TCs, and a heavy branch will lead to a lower TC than a light one. This study is expected to provide some fundamental guidance to obtain a polymer with a low TC.

[DOI: 10.1115/1.4038003]

Keywords: thermal conductivity, polymer, side chain, molecular dynamics simulation, spectral energy density

1 Introduction

Not only a high thermal conductivity (TC) but also a quite low TC is desired for polymers because of their wide applications [1–6], such as a high TC for application as a thermal interface material [7,8] and a low TC for application as a thermal insulation material. Single polymer chains and highly aligned polymer fibers have attracted a wide attention due to their potential high TC [9–16]. Although a single polymer chain may possess a high TC, polymers are generally regarded as a thermal insulator because of their very low thermal conductivities on the order of 0.1 W m^{-1} K^{-1} [17]. One of the reasons for the low TC is that the polymer chains are randomly coiled in the polymers, which effectively shortens the mean free path (MFP) of heat-carrying phonons [18,19]. Another reason is that the TC of these polymers can be significantly influenced by the morphology of individual chains [14–17,20–22]. Besides these two reasons, the method to further decrease the TC of a polymer is still desired to develop a thermal insulator.

There have already been some methods to reduce the TC of a polymer chain. Liao et al. [23] tuned the TC of a polymer chain by atomic mass modifications and found that heavy substituents hinder heat transport substantially. Robbins and Minnich [16] found that even perfectly crystalline polynorbornene has an exceptionally low TC near the amorphous limit due to extremely strong anharmonic scattering. Most recently, Ma and Tian [24] studied the influence of the side chains on the TC of bottlebrush polymers, and predicted that side chains dominate the heat conduction and could lead to a lower TC. Some other studies also shown that chain segment disorder, or the random rotations of segments in a chain, will lead to a lower TC [15,25–28].

In this paper, we take the effect of branches into account to probe a way to reduce the TC of a polymer. Considering the complex structure of a polymer, we just focus on the polyethylene (PE) chain. Results turn out that the TC of a PE chain with branches can be decreased to be only 40% that of a pristine chain. The paper is organized as follows: first, a reverse nonequilibrium molecular dynamics (RNEMD) method is introduced; and then the effects of backbone chain length, branching chain location, branching chain type, and the number density of branching chains are simulated and discussed. This study is expected to provide some fundamental guidance to obtain a polymer with a low TC.

2 Simulation Method

The materials studio is applied to build the initial configuration of the PE chain and the modified PE chain. The PE chain is established by replicating the PE segments which is the unit cell of PE's idealized bulk lattice structure with a length of 2.507 Å. The schematic structures of a pristine PE chain and a PE-ethyl chain are shown in Fig. 1. After building the PE chain, with the COMPASS II potential [29–32], we first relax the system in an NVT (constant number of atoms, temperature, and volume) ensemble at a temperature of 300 K for 125 ps, where the Nose–Hoover thermostat [33,34] is applied to obtain the constant temperature. And then, a NVE (constant number of atoms, volume, and energy) ensemble is used to release the thermal stress. In the simulation process, we double-check that the total energy has reached minimum and becomes unchangeable at the end of NVT and NVE ensembles to make sure that our systems have already been equilibrated.

To calculate TC, the RNEMD [35,36] simulation is performed on the well equilibrated structures to establish a temperature gradient. In the RNEMD method, each of the simulation boxes is divided into several slabs with a periodic boundary in the heat transfer direction. As that shown in Fig. 2, the simulation system is divided into several slabs (20 to 200 slabs, depending on the chain length), slab 0 is the "hot" slab, and the slab N/2 is the "cold" slab. Other slabs are used to obtain the temperature distributions. The heat flux is created by exchanging velocities of particles in cold and hot slabs. The cold slab donates its "hottest" particles (particles with the highest kinetic energy) to the hot slab in exchange for the latter's "coolest" particles (particles with the lowest kinetic energy). Performing this exchange periodically results in the heating up of the hot slab and cooling down of the cold slab. This process eventually yields a steady-state temperature gradient due to thermal conduction through slabs separating the cold and hot slabs. The TC is calculated exactly by the relationship

[1]Corresponding author.

Contributed by the Heat Transfer Division of ASME for publication in the Journal of Heat Transfer. Manuscript received December 30, 2016; final manuscript received July 26, 2017; published online October 25, 2017. Assoc. Editor: Alan McGaughey.

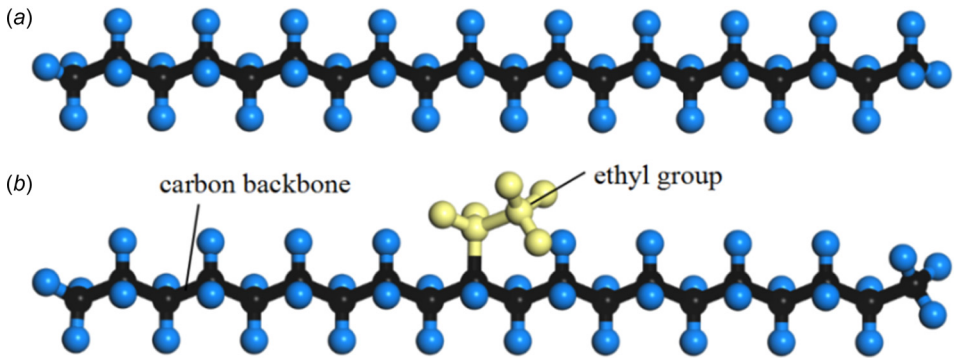

Fig. 1 Schematic structures of PE chains: (*a*) a pristine PE chain with a length of ten segments and (*b*) a PE-ethyl chain

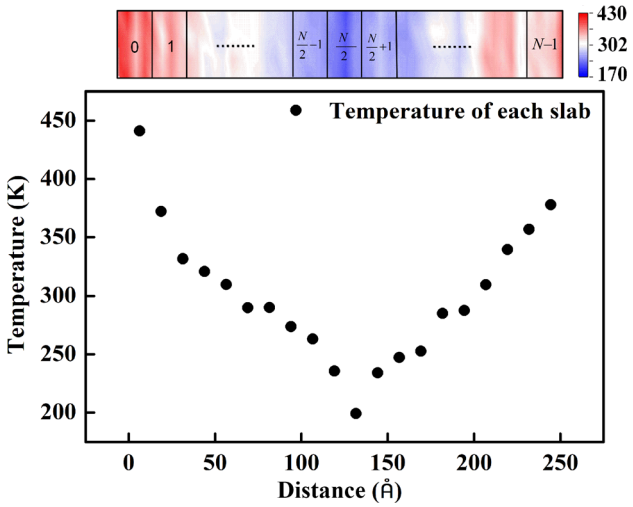

Fig. 2 Temperature distribution of a pristine PE chain with a length of 100 segments (25 nm)

$$\lambda \frac{\sum \frac{m}{2}\left(\nu_h^2 - \nu_c^2\right)}{2tA(\partial T/\partial Z)} \tag{1}$$

where the sum is taken over all transfer events during the simulation time t, m is the mass of the atoms, and ν_c and ν_h are the velocities of the identical mass particles that participate in the exchange procedure from the cold and hot slabs, respectively. A is the cross-sectional area which is selected to be 14.7 Å^2 with a branch-caused uncertainty less than 1.6% as listed in Table 1. Such a small difference between cross-sectional areas will not lead to a large TC difference as that caused by branches (will be discussed later). The TC present in this work could be scaled by a different cross-sectional area for a comparison. With a time-step of 1 fs, a total simulation time of 0.1 ns is taken to get a good linear temperature distribution. The temperature which is adopted to calculate the temperature gradient is averaged through every 1000 simulation steps (1 ps). The temperature fluctuation in the simulation can be reduced by this average method. With heat flux printed out every 0.1 ps, the TC is calculated at the last step. The temperature distribution in a PE chain with a length of 100 segments is shown in Fig. 2 as an example. The linear temperature region is fitted to obtain the temperature gradient for the calculation of the effective TC by using the Fourier's law. The TC calculated at different simulation times is shown in Fig. 3. It shows that 0.1 ns is long enough to get a converged TC.

Table 1 Cross-sectional areas (Å^2) used in the TC calculation

	50 segments	75 segments	100 segments
Pristine PE	14.502	14.469	14.539
PE-ethyl	14.872	14.717	14.697
PE-benzene	14.718	14.902	14.890
PE-phenoxy	14.858	14.750	14.822
PE-ethoxy	14.717	14.848	14.730
PE-methoxy	14.741	14.729	14.601
PE-ethylene	14.769	14.650	14.671
PE-hydroxy	14.524	14.649	14.561

3 Results and Discussion

First, the length dependence of the TC of a pristine PE chain is investigated and compared with that in early researches. And then, the TC of the pristine PE chains with different lengths is compared with that of a PE-ethyl chain. Third, the effect of the branch arrangement is considered. Finally, the influence of the branch type and the number density of branches are taken into account.

3.1 Length Dependence of TC. Thermal conductivities of the pristine PE chain with different chain lengths at 300 K are first simulated and presented in Fig. 4(*a*). Previous works [14,37,38] about the pristine PE chains are also added in Fig. 4(*a*) for comparison. As that shown in Fig. 4(*a*), there is an obvious increase of the TC with the increase of the chain length. Even with the length increasing to be 200 nm, the TC still not converges, which suggests that some portion of the phonons can still travel ballistically

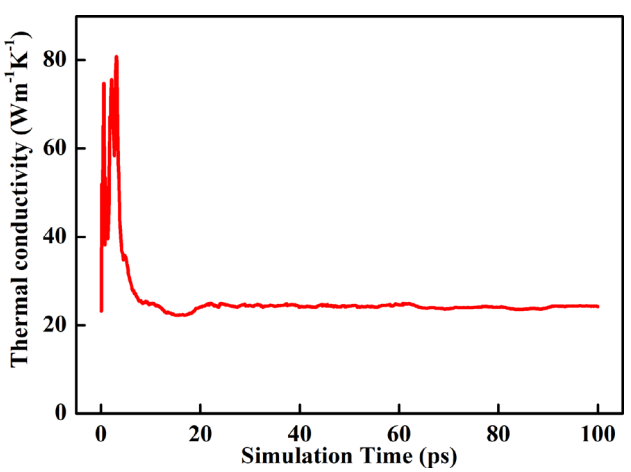

Fig. 3 TC of a pristine PE chain with a length of 100 segments

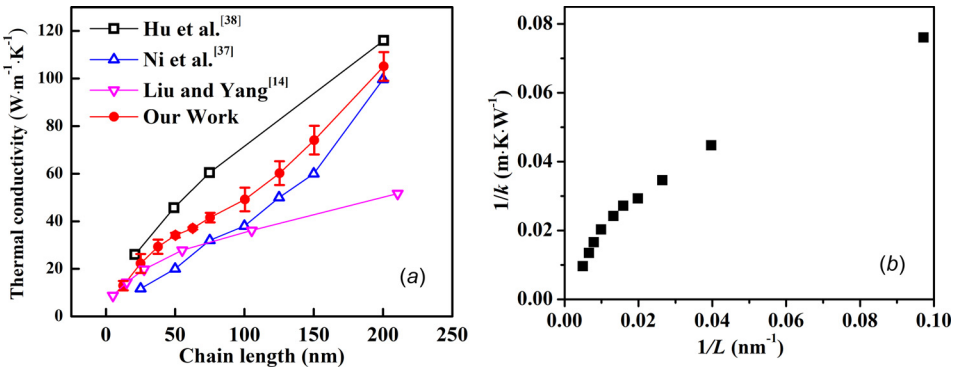

Fig. 4 TC of a pristine PE chain: (*a*) compared with results simulated by Ni et al. [37], Hu et al. [38], and Liu and Yang [14] and (*b*) inverse of the TC plotted against the inverse of the chain length

in such a length. Our simulation work confirms that the TC of a pristine PE chain will increase with the increasing number of segments (or chain length), and the TC of a single PE chain is several orders of magnitude larger than that of a PE polymer. In Fig. 4(*a*), the TC difference between different works should be attributed to the application of different simulation methods, considering that the nonequilibrium molecular dynamics method is applied in our and the work of Hu et al. and the equilibrium molecular dynamics method is utilized in the work of Ni et al. and Liu and Yang. It seems that a nonequilibrium molecular dynamics method will give a higher TC than an equilibrium molecular dynamics method. This was also noticed in other studies [39,40], and some explanations can be found there.

Plotting $1/k$ against $1/L$ in Fig. 4(*b*), we can see that with the increase of $1/L$, the $1/k$ first increases rapidly and then saturates to a linear increase. The method by extrapolating the linear relationship between the inverse of the TC ($1/k$) and the inverse of the sample length ($1/L$) to get the TC with an infinite length fails. This failure is attributed to the divergent thermal conductivity at $1/L \to 0$ where $1/k \to 0$, which has already been carefully studied and explained with theoretical and molecular dynamics methods in Ref. [41], more details can be found there.

Thermal conductivities of the pristine PE chain and the PE-ethyl chain with lengths ranging from 100 to 500 segments (or 25.07–125.35 nm) are compared in Fig. 5. It turns out that both TCs of the pristine PE chain and the PE-ethyl chain increase with the increasing length, and the TC of a PE-ethyl chain is only about 75% that of a pristine PE chain. To illustrate the underlying mechanism of the lower TC of the PE-ethyl chain, the vibrational density of states (VDOS) is calculated by using the Fourier transform of the velocity autocorrelation function. Results are compared between the pristine PE chain and the PE-ethyl chain with 50 segments, as shown in Fig. 6. Considering the low-frequency (<20 THz) phonons dominate the TC due to their high group velocities and long MFPs [23], the lower VDOS of the PE-ethyl chain in the low frequency should be responsible for the lower TC, where the branch acts as a center of low-frequency-phonon scattering.

To further illustrate the phonon scattering caused by the branching chains, the phonon spectral energy density (SED) of the pristine PE and PE-ethyl chains is calculated based on the velocity output of MD simulations. The atomic velocities are obtained by a NVE simulation at a temperature of 300 K. The frequency resolution is selected to be 0.01 THz with 0.1 ns NVE simulations, and the wave-number is $0.02\kappa/(2\pi/a)$, where $\kappa = 2\pi n/aN$, here a is the lattice constant, N is the total number of unit cells along the heat transfer direction ($N = 50$ in this work), and n is an integer ranging from 0 to $N-1$. More details about the calculation can be found in Refs. [42–45]. Results are shown in Fig. 7 with the shading signifying the magnitude of the SED. The SED of a pristine PE chain in Fig. 7(*a*) coincides with that in Ref. [16] which confirms the reliability of our calculation. For each phonon mode in Fig. 7, the range of frequencies is related to the anharmonicity of the potential and the rate of the phonon scattering. The situation when branch atoms move far away from equilibrium positions may lead to a significant broadening of the peaks in Fig. 7. Fitting the shape of peak and valley profiles of SED at all branches to the Lorentzian function [42–45], the phonon relaxation time is obtained and shown in Fig. 8. It shows that the magnitude of the phonon relaxation time is greatly reduced by branching chains, which should be

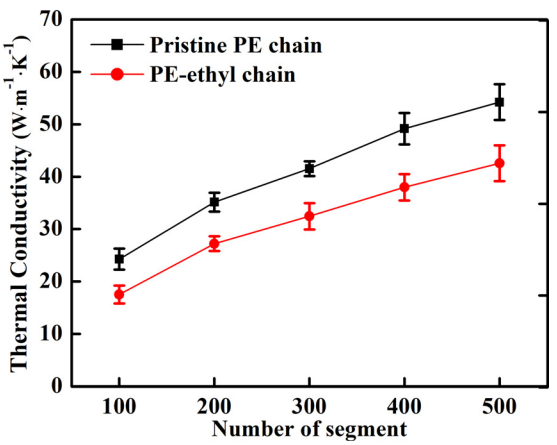

Fig. 5 Length dependence of TCs of the PE chain and the PE-ethyl chain

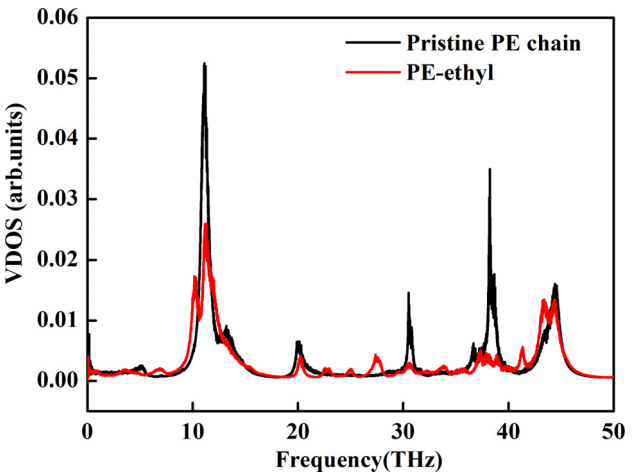

Fig. 6 VDOS of the PE and PE-ethyl chains

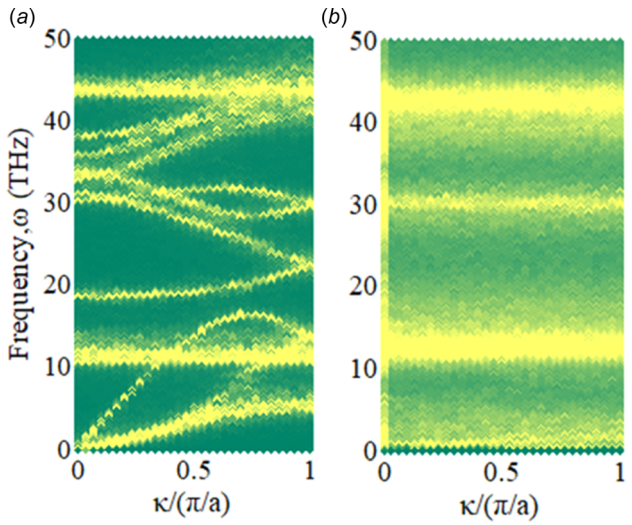

Fig. 7 SEDs of a pristine PE chain (*a*) and a PE-ethyl chain with a branch number density of one branch per ten segments (*b*). The shading signifies the magnitude of the SED.

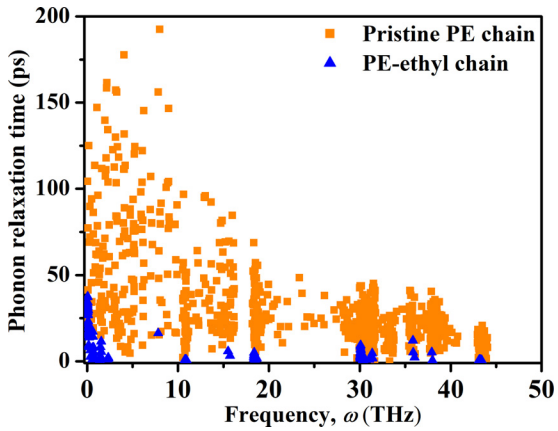

Fig. 8 The phonon relaxation times in a pristine PE chain and a PE-ethyl chain

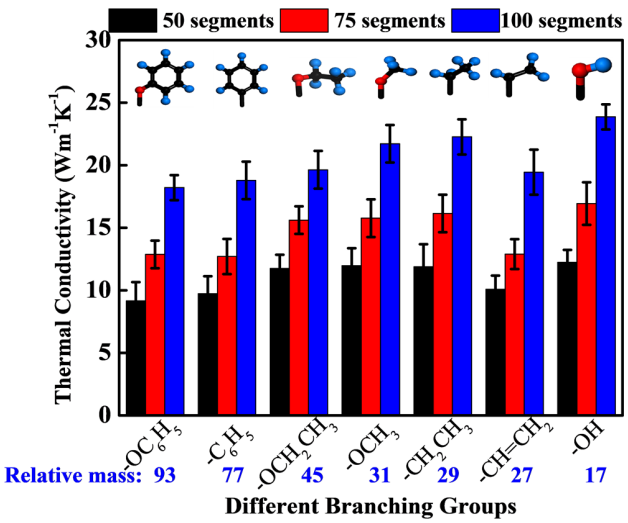

Fig. 10 TCs of PE chains with different types of branches

responsible for the lower TC of the PE-ethyl chain. The redistribution of phonons and the smearing acoustic branches of the PE-ethyl chain in Fig. 7(*b*) proves the result in Fig. 8 that there is a more severe phonon scattering for a PE-ethyl chain than a pristine PE chain.

3.2 Influence of Branch Arrangements. The influence of branch locations is considered in this part. For a pristine PE chain, there are different locations from the simulation region boundary to the branching ethyl. Five special locations are selected to branch a short chain, labeled as P1, P2, P3, P4, and P5, respectively, as that shown in Fig. 9(*a*). The result in Fig. 9(*b*) confirms that the presence of a branching chain can truly reduce the TC, and the average TC of a PE-ethyl chain is about 0.7 times that of a pristine PE chain. Our simulations also indicate that there is almost a same TC for different locations in Fig. 9(*b*). This is attributed to the periodic boundary condition in the simulation. The small TC discrepancies between different locations should be caused by the different distance of the branch from the simulation boundary. If the boundary and the branching chains are both thought as defects on a pristine PE chain, the TC with ethyl located at the middle of the chain (P1) will be lower than other TCs (P2, P3, P4, and P5), because of the small distance from the

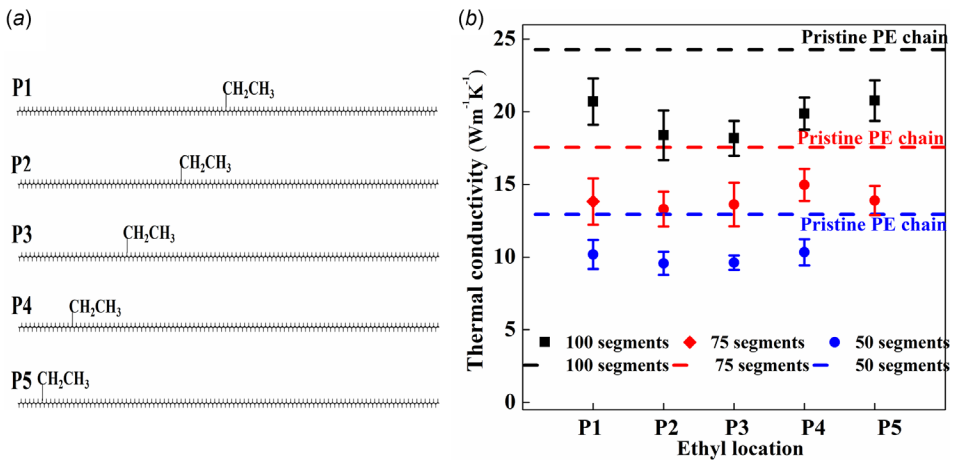

Fig. 9 TC of the PE-ethyl chain with different branch locations: (*a*) structures with 100 segments used in the simulation and (*b*) effect of branch locations on the TC. Dashed lines stand for the pristine PE chains.

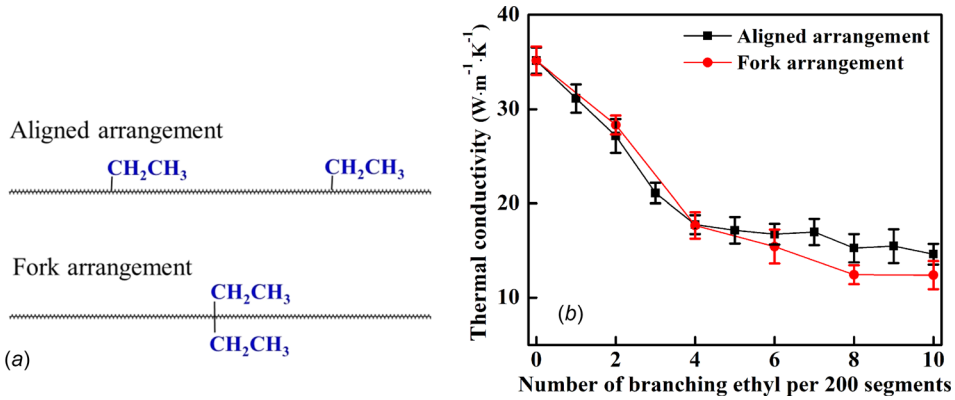

Fig. 11 TC of a PE chain with different number density of branches: (*a*) two special branch arrangements (only a part is shown here) and (*b*) TC comparison between two arrangements

middle of the chain to the system boundary. This is confirmed by results in Fig. 9(*b*).

3.3 Influence of Branching Chain Types and Number Density of Branches. Seven different types of short chains are branched on the middle segment of a PE chain, respectively, for comparisons. They are different from the weight and the type of chemical bonds between the backbone and the branch, as shown in Fig. 10, which are listed as phenoxy group, phenyl group, ethoxy group, methoxy group, ethyl group, ethylene group, and hydroxy group, respectively. The black, red, and blue columns in Fig. 10 stand for different chain lengths. The relative masses of different branches are also shown in Fig. 10. We can see that all types of branches can lead to a decrease of TC, and a heavy branch leads to a lower TC than a light one, except for the ethylene group for which TC may be further decreased by a different bond. It agrees with the conclusion in Ref. [23] that a chain modified by a heave atom possesses a lower TC than that modified by a light one, where the modifying atom can be thought a special short branch. We conclude that different branches will lead to a different decrease of thermal conductivities because of the different weights. More studies are still needed to probe the effect of bonds between the backbone and the branch on the TC.

The effect of the number density of branches is studied in this part. The number density of branches is defined as the number of branches divided by the number of PE segments. Two hundred segments (50.14 nm) are applied as a periodic unit in the simulation, and the ethyl group is selected as the branch. Considering there are different locations on a PE chain to branch an ethyl group, we only consider two special location arrangements, i.e., the aligned arrangement and the fork arrangement, as that shown in Fig. 11(*a*). For the aligned arrangement of ten branching ethyl, they are equally distributed on the PE chain, only a part of the chain is shown in Fig. 11(*a*); for the fork arrangement of ten branching ethyl, every two branching ethyl are located at the same segment of the PE chain, as that shown in Fig. 11(*a*). The corresponding TC of these two arrangements is shown in Fig. 11(*b*). It shows that a larger number density of branches leads to a lower TC for both arrangements. With an increase of the number density of branches, the TC of a PE-ethyl chain finally converges to be only about 40% that of the pristine PE chain. This can be understood by that with the increase of the number density, the distance between branches is reduced, and the long-MFP phonons will be decreased until the TC converges to a constant value. It can be predicted that if a PE-ethyl chain instead of a pristine PE chain is used to build up a polymer, the TC of the polymer will be much reduced, because of the lower TC of the PE-ethyl chain and the additional mass of branches. What kind of a chain will lead to a lower TC is the key point of this paper, and more studies are still needed to figure out the effect of long branches on the TC of a pristine chain [24].

4 Conclusions

It is desirable to further reduce the TC of a polymer for developing a thermal insulation material. In this paper, we take branches into account to probe a way to reduce the TC of a chain. With the RNEMD method, the TCs of the pristine PE chain and the PE-ethyl chain are simulated and compared. Influences of the chain length, branch arrangements, types, and number density of branches are considered. Our results suggest that the branch has a positive effect to reduce the TC of a PE chain. If the number density of ethyl branches becomes larger than eight ethyls per 200 segments, the TC of a PE-ethyl chain converges to be only about 40% that of a pristine PE chain. This conclusion will not be influenced by the branch arrangements. Different branches cause a different decrease of thermal conductivities because of their different weights, and a heavy branch leads to a lower TC than a light one. This study is expected to provide some fundamental guidance to obtain a polymer with a low TC.

Funding Data

- National Natural Science Foundation of China (Grant No. 51406224).

References

[1] Li, G., Shrotriya, V., Yao, Y., Huang, J., and Yang, Y., 2007, "Manipulating Regioregular Poly (3-Hexylthiophene): [6,6]-Phenyl-C61-Butyric Acid Methyl Ester Blends-Route Towards High Efficiency Polymer Solar Cells," J. Mater. Chem., **17**(30), pp. 3126–3140.
[2] Nie, Z., and Kumacheva, E., 2008, "Patterning Surfaces With Functional Polymers," Nat. Mater., **7**(4), pp. 277–290.
[3] Liu, C., 2007, "Recent Developments in Polymer MEMS," Adv. Mater., **19**(22), pp. 3783–3790.
[4] Ryan, A. J., 2008, "Nanotechnology: Squaring Up With Polymers," Nature, **456**(7220), pp. 334–336.
[5] Bruening, M., and Dotzauer, D., 2009, "Polymer Films: Just Spray It," Nat. Mater., **8**(6), pp. 449–450.
[6] Charnley, M., Textor, M., and Acikgoz, C., 2011, "Designed Polymer Structures With Antifouling-Antimicrobial Properties," React. Funct. Polym., **71**(3), pp. 329–334.
[7] Han, Z., and Fina, A., 2011, "Thermal Conductivity of Carbon Nanotubes and Their Polymer Nanocomposites: A Review," Prog. Polym. Sci., **36**(7), pp. 914–944.
[8] Singh, V., Bougher, T. L., Weathers, A., Cai, Y., Bi, K., Pettes, M. T., McMenamin, S. A., Lv, W., Resler, D. P., Gattuso, T. R., Altman, D. H., Sandhage, K. H., Shi, L., Henry, A., and Cola, B. A., 2014, "High Thermal Conductivity of Chain-Oriented Amorphous Polythiophene," Nat. Nanotechnol., **9**(5), pp. 384–390.
[9] Henry, A., and Chen, G., 2008, "High Thermal Conductivity of Single Polyethylene Chains Using Molecular Dynamics Simulations," Phys. Rev. Lett., **101**(23), p. 235502.
[10] Cao, B. Y., Li, Y. W., Kong, J., Chen, H., Xu, Y., Yung, K.-L., and Cai, A., 2011, "High Thermal Conductivity of Polyethylene Nanowire Arrays Fabricated by an Improved Nanoporous Template Wetting Technique," Polymer, **52**(8), pp. 1711–1715.

[11] Henry, A., Chen, G., Plimpton, S. J., and Thompson, A., 2010, "1D-to-3D Transition of Phonon Heat Conduction in Polyethylene Using Molecular Dynamics Simulations," Phys. Rev. B, **82**(14), p. 144308.
[12] Jiang, J. W., Zhao, J., Zhou, K., and Rabczuk, T., 2012, "Superior Thermal Conductivity and Extremely High Mechanical Strength in Polyethylene Chains From Ab Initio Calculation," J. Appl. Phys., **111**(12), p. 124304.
[13] Shen, S., Henry, A., Tong, J., Zheng, R., and Chen, G., 2010, "Polyethylene Nanofibres With Very High Thermal Conductivities," Nat. Nanotechnol., **5**(4), pp. 251–255.
[14] Liu, J., and Yang, R., 2012, "Length-Dependent Thermal Conductivity of Single Extended Polymer Chains," Phys. Rev. B, **86**(10), p. 104307.
[15] Luo, T., Esfarjani, K., Shiomi, J., Henry, A., and Chen, G., 2011, "Molecular Dynamics Simulation of Thermal Energy Transport in Polydimethylsiloxane (PDMS)," J. Appl. Phys., **109**(7), p. 074321.
[16] Robbins, A. B., and Minnich, A. J., 2015, "Crystalline Polymers With Exceptionally Low Thermal Conductivity Studied Using Molecular Dynamics," Appl. Phys. Lett., **107**(20), p. 201908.
[17] Umur, A., Gemert, M. J. C. V., and Ross, M. G., 1986, *Introduction to Physical Polymer Science*, Wiley, Hoboken, NJ.
[18] Hu, Y., Zeng, L., Minnich, A. J., Dresselhaus, M. S., and Chen, G., 2015, "Spectral Mapping of Thermal Conductivity Through Nanoscale Ballistic Transport," Nat. Nanotechnol., **10**(8), pp. 701–706.
[19] Zeng, L., Collins, K. C., Hu, Y., Luckyanova, M. N., Maznev, A. A., Huberman, S., Chiloyan, V., Zhou, J., Huang, X., Nelson, K. A., and Chen, G., 2015, "Measuring Phonon Mean Free Path Distributions by Probing Quasiballistic Phonon Transport in Grating Nanostructures," Sci. Rep., **5**(1), p. 17131.
[20] Henry, A., and Chen, G., 2009, "Anomalous Heat Conduction in Polyethylene Chains: Theory and Molecular Dynamics Simulations," Phys. Rev. B, **79**(14), p. 144305.
[21] Sasikumar, K., and Keblinski, P., 2011, "Effect of Chain Conformation in the Phonon Transport Across a Si-Polyethylene Single-Molecule Covalent Junction," J. Appl. Phys., **109**(11), p. 114307.
[22] Savin, A. V., and Savina, O. I., 2014, "Dependence of the Thermal Conductivity of a Polymer Chain on Its Tension," Phys. Solid State, **56**(8), pp. 1664–1672.
[23] Liao, Q., Zeng, L., Liu, Z., and Liu, W., 2016, "Tailoring Thermal Conductivity of Single-Stranded Carbon-Chain Polymers Through Atomic Mass Modification," Sci. Rep., **6**(1), p. 34999.
[24] Ma, H., and Tian, Z., 2017, "Effects of Polymer Topology and Morphology on Thermal Transport: A Molecular Dynamics Study of Bottlebrush Polymers," Appl. Phys. Lett., **110**(9), p. 091903.
[25] Zhang, T., Wu, X., and Luo, T., 2014, "Polymer Nanofibers With Outstanding Thermal Conductivity and Thermal Stability: Fundamental Linkage Between Molecular Characteristics and Macroscopic Thermal Properties," J. Phys. Chem. C, **118**(36), pp. 21148–21159.
[26] Zhang, L., Ruesch, M., Zhang, X., Bai, Z., and Liu, L., 2015, "Tuning Thermal Conductivity of Crystalline Polymer Nanofibers by Interchain Hydrogen Bonding," RSC Adv., **5**(107), pp. 87981–87986.
[27] Zhang, T., and Luo, T., 2012, "Morphology-Influenced Thermal Conductivity of Polyethylene Single Chains and Crystalline Fibers," J. Appl. Phys., **112**(9), p. 094304.
[28] Ma, H., and Tian, Z., 2015, "Effects of Polymer Chain Confinement on Thermal Conductivity of Ultrathin Amorphous Polystyrene Films," Appl. Phys. Lett., **107**(7), p. 073111.
[29] Luo, T., and Lloyd, J. R., 2012, "Enhancement of Thermal Energy Transport Across Graphene/Graphite and Polymer Interfaces: A Molecular Dynamics Study," Adv. Funct. Mater., **19**(12), pp. 587–596.
[30] Sun, H., 1998, "COMPASS: An Ab Initio Force-Field Optimized for Condensed-Phase Applications Overview With Details on Alkane and Benzene Compounds," J. Phys. Chem. B, **102**(38), pp. 7338–7364.
[31] Sun, H., Ren, P., and Fried, J. R., 1998, "The COMPASS Force Field: Parameterization and Validation for Phosphazenes," Comput. Theor. Polym. Sci., **8**(1–2), pp. 229–246.
[32] Rigby, D., Sun, H., and Eichinger, B. E., 1997, "Computer Simulations of Poly (Ethylene Oxide): Force Field, PVT Diagram and Cyclization Behavior," Polym. Int., **44**(3), pp. 311–330.
[33] Nose, S., 1984, "A Unified Formulation of the Constant Temperature Molecular Dynamics Methods," Rev. Faith Int. Affairs, **81**(1), p. 511.
[34] Hoover, W. G., 1985, "Canonical Dynamics: Equilibrium Phase-Space Distributions," Phys. Rev. A, **31**(3), pp. 1695–1697.
[35] Müllerplathe, F., 1997, "A Simple Nonequilibrium Molecular Dynamics Method for Calculating the Thermal Conductivity," J. Chem. Phys., **106**(14), p. 6082.
[36] Huang, C., Wang, Q., and Rao, Z., 2015, "Thermal Conductivity Prediction of Copper Hollow Nanowire," Int. J. Therm. Sci., **94**, pp. 90–95.
[37] Ni, B., Watanabe, T., and Phillpot, S. R., 2009, "Thermal Transport in Polyethylene and at Polyethylene-Diamond Interfaces Investigated Using Molecular Dynamics Simulation," J. Phys.: Condens. Matter, **21**(8), p. 084219.
[38] Hu, G. J., Cao, B. Y., and Li, Y. W., 2014, "Thermal Conduction in a Single Polyethylene Chain Using Molecular Dynamics Simulations," Chin. Phys. Lett., **31**(8), p. 086501.
[39] Termentzidis, K., Merabia, S., Chantrenne, P., and Keblinski, P., 2011, "Cross-Plane Thermal Conductivity of Superlattices With Rough Interfaces Using Equilibrium and Non-Equilibrium Molecular Dynamics," Int. J. Heat Mass Transfer, **54**(9), pp. 2014–2020.
[40] Landry, E. S., Hussein, M. I., and McGaughey, A. J. H., 2008, "Complex Superlattice Unit Cell Designs for Reduced Thermal Conductivity," Phys. Rev. B, **77**(18), p. 184302.
[41] Hu, L., Evans, W. J., and Keblinski, P., 2011, "One-Dimensional Phonon Effects in Direct Molecular Dynamics Method for Thermal Conductivity Determination," J. Appl. Phys., **110**(11), p. 113511.
[42] Qian, X., Gu, X. K., and Yang, R. G., 2016, "Lattice Thermal Conductivity of Organic-Inorganic Hybrid Perovskite CH3NH3PbI," Appl. Phys. Lett., **108**(6), p. 063902.
[43] Li, C. J., Li, G., and Zhao, H. J., 2015, "Thermal Conductivity Variation of Graphene With Patterned Double-Side Hydrogen Doping," J. Appl. Phys., **118**(7), p. 075102.
[44] Thomas, J. A., Turney, J. E., Iutzi, R. M., Amon, C. H., and McGaughey, A. J., 2010, "Predicting Phonon Dispersion Relations and Lifetimes From the Spectral Energy Density," Phys. Rev. B, **81**(8), p. 081411.
[45] Feng, T., Qiu, B., and Ruan, X., 2015, "Anharmonicity and Necessity of Phonon Eigenvectors in the Phonon Normal Mode Analysis," J. Appl. Phys., **117**(19), p. 195102.